ISSN 0869-5911, Petrology, 2009, Vol. 17, No. 6, pp. 523–536. © Pleiades Publishing, Ltd., 2009.
Original Russian Text © S.A. Silantyev, M.V. Mironenko, A.A. Novoselov, 2009, published in Petrologiya, 2009, Vol. 17, No. 6, pp. 563–577.

Hydrothermal Systems Hosted in Peridotites at Slow-Spreading Ridges. Modeling Phase Transformations and Material Balance: Upwelling Limb of the Hydrothermal Cell

S. A. Silantyev, M. V. Mironenko, and A. A. Novoselov

Vernadsky Institute of Geochemistry and Analytical Chemistry, Russian Academy of Sciences, ul. Kosygina 19, Moscow, 119991 Russia

e-mail: silantyev@geokhi.ru

Received September 22, 2009; in final form, December 10, 2008

Abstract—The research was centered on the estimation of geochemical and mineralogical effects related to the transport of hydrothermal fluid to the seafloor surface in the upwelling limb of a hydrothermal system hosted in peridotites at slow-spreading mid-oceanic ridges. The three variants of the location of the root zone of the circulation cell considered in this research were as follows: (1) shallow-depth, with $T = 107°C$, $P = 1.14$ kbar; (2) moderate low depths, with $T = 151°C$, $P = 1.4$ kbar; and (3) deep, with $T = 500°C$, $P = 4$ kbar. The modeling results demonstrate that ore material is accumulated in the discharge zones of serpentinite-related hydrothermal systems only at a high temperature of the fluid in the discharge zone of the upwelling limb of the circulation cell. The root zones at hydrothermal fields that meet this condition should be situated at a significant depth in the crustal section. It was also established that a significant volume of ore material involved in hydrothermal material exchange between the peridotites and fluid is redeposited in the downwelling limb of the hydrothermal system and gives rise to disseminated ore mineralization, which is typical of many serpentinized abyssal peridotites. The activity of moderately low-temperature and low-temperature hydrothermal systems in peridotites does not concentrate ore material in the discharge zone, and no hydrothermal edifices can grow at such systems.

DOI: 10.1134/S0869591109060010

INTRODUCTION

Our recently published paper (Silanyev et al., 2009) proposed a geodynamic model for the origin of a hydrothermal system in peridotites in a slow-spreading mid-oceanic ridge. Using geochemical simulation techniques, we reproduced phase and chemical transformations in peridotites in the course of seawater-derived fluid percolation through the vertical section (Hess crust). This allowed us to model mineralogical and chemical effects in the downwelling limb of a circulation hydrothermal cell. This publication is a continuation of the aforementioned paper and is devoted to modeling mineral and chemical transformations related to the evolution of hydrothermal solution in the upwelling limb of the cell.

Available data lead to the conclusion that hydrothermal systems of mid-oceanic ridges (MOR) are characterized by similar structures of their circulation cells (regardless of the host crustal rocks), which include the following elements: (1) a downwelling limb, (2) a root (or reaction) zone, and (3) an upwelling limb with a discharge zone at the mouth of the hydrothermal vent. Inasmuch as we modeled process in the upwelling limb of the hydrothermal system, we considered the part of the hydrothermal cell between the reaction (root) zone and the discharge zone, according to the classification (German and Von Damm, 2003; Tivey, 2007). The root zone of a hydrothermal cell is characterized by the highest temperature and pressure, which correspond to the *P–T* parameters of the host rocks or the roof of the magma chamber. The latter acts as a heat source for the hydrothermal system and sometimes also as a source of gases dissolved in the fluid (predominantly CO_2 and He) (German and Van Damm, 2003). Upon reaching conditions corresponded to the boiling line, fluid in this zone can undergo phase separation and form NaCl-enriched, predominantly aqueous and vapor-saturated hydrothermal fluids that have different densities (Von Damm et al., 1997; Grichuk, 2000; German and Von Damm, 2003; Tivey, 2007). As a result of phase separation, volatiles predominantly enrich the vapor phase (Von Damm, 1995), and the effect of phase separation is likely responsible for the occurrence of hydrothermal vents at the seafloor, with Cl concentrations in these vents being much higher or much lower than in seawater (Von Damm, 1995). The fluid thus generated in the root zone has a very high buoyancy compared with cold seawater and thus rapidly ascends to the seafloor surface. As follows from available empirical and calculation data, the fluid ascends to the surface too rapidly to reach thermodynamic and chemical equilibrium with the host rocks (Tivey, 2007). The only possible exception can be such fluid components as Si, H_2(aq), and Cu, whose behavior in the upwelling limb of a hydro-

thermal system can be explained by reaching local equilibrium (Von Damm, 1995).

It should be mentioned that, due to the absence of empirical information on the structure of the root zone and the composition of the hydrothermal fluid penetrating it, modern hypotheses concerning the character of processes and material balance at this level can be based mostly on experimental data and simulation results.

In the discharge zone of hydrothermal fluid, the fluid mixes with seawater, and material precipitating from it forms various topographic features and edifices: sulfide chimneys, diffusers, mats, and crusts. The mineral composition of these edifices depends on the chemical composition of the hydrothermal fluid and the mixing parameters of the fluid with seawater (Haymon, 1983; Tivey and McDuff, 1990; Peng and Zhou, 2005). Compared with the vast volume of data on the mineralogy and inner structure of hydrothermal edifices at active hydrothermal fields on basalts at MOR, information on analogous edifices on peridotites in slow-spreading MOR is still scarce and pertains only to a few active hydrothermal fields in the Central Atlantic: Ashadze, Logachev, Lost City, Rainbow, and Saldanha. Obviously, sulfide edifices at high-temperature hydrothermal fields on peridotites (Ashadze, Logachev, and Rainbow) are formed, similar to ore chimneys of typical black smokers in association with basalts, during the mixing of hydrothermal fluid and seawater at high fluid/seawater ratios. Sulfide chimneys of active fields related to peridotites are zonal. It should be mentioned that, judging from available data, the mineralogical zoning of individual ore edifices on peridotites resembles the zoning in the chimneys of black smokers related to basalts. For example, chimneys at the Rainbow field have an outermost zone of massive fine-grained sphalerite and chalcopyrite with chalcosine, bornite, and covellite, whereas the inner zones of the chimneys are dominated by Cu and Fe sulfides (Vikent'ev, 2004). At the same time, the chimneys of black smokers related to basalts usually contain an inner zone of massive Cu–Fe sulfides and an outer zone of chalcopyrite, pyrrhotite, pyrite, and sphalerite (Haymon, 1983; Peng and Zhou, 2005; Tivey, 2007). It is thought that the chimney of a classic black smoker (related to basalts) is formed in two stages (Haymon, 1983; Bogdanov, 1997; Tivey and McDuff, 1990). During the first stage (sulfate formation, according to Peng and Zhou, 2005), anhydrite and caminite $Mg(OH, SO_4)H_2O$ (Haymon, 1983) crystallize from seawater heated to >130°C (Bogdanov, 1997) around hydrothermal jets on the seafloor. The outer porous zone of the smoker chimney constrains fluid mixing with seawater, and sulfides are deposited within the anhydrite shell at fluid-dominated conditions during the second stage (sulfide formation, according to Peng and Zhou, 2005). Minerals are precipitated in the following sequence, depending on the extent of mixing of the hydrothermal fluid and seawater (Haymon, 1983): chalcopyrite ⟶ bornite ⟶ chalcosine ⟶ covellite. The outer (sulfate) zone of the hydrothermal edifice may contain (along with pyrite and sphalerite) also minor amounts of silicates: amorphous silica and talc (Haymon, 1983). Hence, the opposite migration of seawater and hydrothermal fluid through the porous outer zone of the hydrothermal edifice controls the development of the concentric zoning in the distribution of solid mineral phases from the highest temperature ones in the central zone to the lowest temperature one in the peripheral part. Hydrothermal fields on peridotites at MAR are highly heterogeneous in terms of physicochemical parameters of the related hydrothermal fluids. They include, along with high-temperature hydrothermal jets (for example, 365°C at the Rainbow field; Douville et al., 2002), the unique Lost City hydrothermal field, at which fluids discharged at the seafloor have temperatures no higher than 40–90°C (Kelley et al., 2005). The walls of hydrothermal spires at this field consist of brucite, aragonite, and serpentine (Dubinina et al., 2007; Lein et al., 2007). Still lower temperatures (7–9°C) were measured in the hydrothermal fluid percolating through the thin layer of foraminiferal ooze overlying the serpentinite massif of Saldanha Seamount at the Saldanha hydrothermal field (Dias and Barriga, 2006). The mineral association of hydrothermal genesis consists there of sulfides, nontronite (a mineral of the montmorillonite group), and poorly crystalline Mn hydroxides. Sediments near hydrothermal jets at the Saldanha field contain Cu, Zn, and Fe sulfides (microchimneys contain isocubanite and sphalerite) and brucite (Dias and Barriga, 2006). The hydrothermally altered sediments at the Saldanha field may contain significant concentrations of Mn, Mg, Fe, Cu, Ni, Cr, and Co. It was hypothesized (Dias and Barriga, 2006) that the unusual geochemical and mineralogical features of the Saldanha field testify that the hydrothermal fluid intensely mixes with fresh seawater.

The diversity of the mineralogical types of hydrothermal edifices in the fluid discharge zone at the seafloor surface composed of peridotites likely reflects differences in the physicochemical parameters of the hydrothermal fluid and the depth of the root zone of the hydrothermal system. The principal goal of our simulations was to evaluate the geochemical and mineralogical effects related to the transport of hydrothermal fluid to the seafloor surface at variable depths of the root zone of the hydrothermal circulation cell in peridotites.

SIMULATION TECHNIQUES

Our earlier paper (Silantyev et al., 2009) reported the results of our simulations of downwelling seawater-derived fluid filtration through mantle peridotites (spinel harzburgites). The whole vertical section of the peridotites was subdivided into 22 blocks with certain *P–T* parameters through which fluid portions (twelve "waves") were successively passed. Interactions between the fluid and minerals of the rocks were ana-

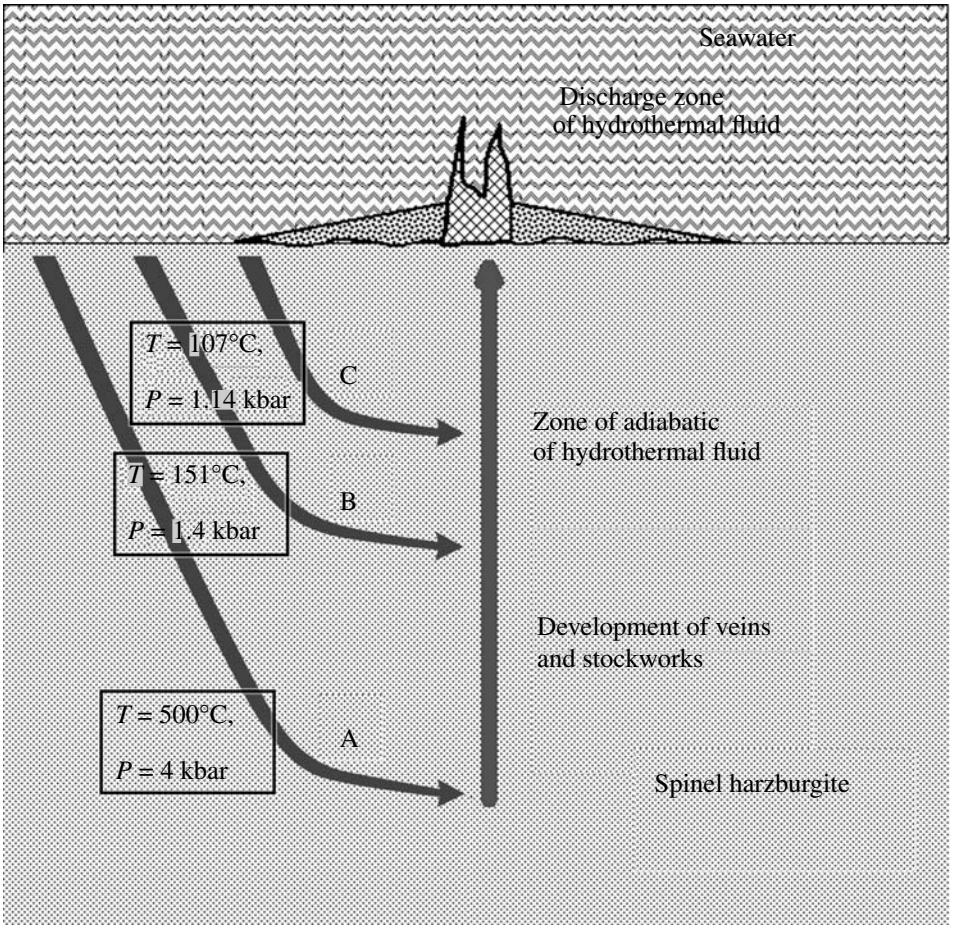

Fig. 1. Schematic representation of the upwelling limb of the peridotite–hydrothermal fluid system.
A—root zone of the hydrothermal cell situated at a depth of approximately 11 km, B—same at a depth of about 3 km, C—same at a depth of 2 km. Cross hatching shows hydrothermal edifices, speckled areas correspond to hydrothermal precipitates.

lyzed in each block with regard for the kinetics of mineral distribution. This paper reports results of our simulations of the upwelling limb. We used compositions of fluid that enters the root zone as the second "wave", because a stationary regime of the system is reached during this "wave". In contrast to the model for the downwelling limb, here we consider the filtration of a single portion of hydrothermal fluid from the root zone to the discharge zone. We have analyzed three possible variants of the depth of the root zone of a hydrothermal circulation cell: (1) shallow depths and $T = 107°C$, $P = 1.14$ kbar; (2) moderate depths and $T = 151°C$, $P = 1.4$ kbar; and (3) significant depths and $T = 500°C$, $P = 4$ kbar (Figs. 1, A, B, and C). The fluid compositions corresponding to these variants of the root zone are listed in Table 1.

Simulations of Chemical Interactions

The chemical transformations of the fluid with variations in the *P–T* parameters and in the course of mixing of the hydrothermal fluid and seawater were simulated as a series of isobaric–isothermal equilibria. It was thereby assumed that the fluid does not have enough time to react with the host rocks and minerals that crystallized previously. We considered only the processes of precipitation and gas release. As in our earlier paper, the simulations were carried out by the GEOCHEQ software package (Mironenko et al., 2000). The system was assumed to consist of 14 components: O–H–Si–Al–Mg–Fe–Ca–Na–Cl–S–C–Zn–Pb–Cu. The gas phase presumably consisted of six components: CH_4, CO, H_2, H_2O, CO_2, and O_2. The fugacity coefficients of the gases were calculated by the Peng–Robinson equation. The possible ore phases were pyrrhotite, sphalerite, chalcopyrite, chalcosine, bornite, galena, pyrite, covellite, and native copper. The following complexes of ore elements were taken into account for the fluid: $CuCl^0$, $Cu(HS)_2^-$, $Cu(OH)_2^-$, Cu^+, $CuCl^+$, Cu^{+2}, $CuCl_2^-$, $CuCl_2^0$, $CuCl_3^-$, $CuCl_4^{-2}$, $CuHS^0$, CuO^0, CuO_2^{-2}, $CuOH^0$, $CuOH^+$, $HCuO_2$, $HZnO_2^-$, $ZnOH^+$, Zn^{+2}, $ZnCl^+$, $ZnCl_2^0$, $ZnCl_3^-$, ZnO^0, ZnO_2^{-2}, $HPbO_2^-$,

Table 1. Composition (mol/kg of H_2O) of the starting hydrothermal fluid ascending from the root zones situated at various depths in the oceanic crust

Component	T = 107°C, P = 1.14 kbar	T = 151°C, P = 1.46 kbar	T = 500°C, P = 4 kbar
ΣCO_2	1.05×10^{-06}	1.75×10^{-17}	4.35×10^{-12}
CH_4	2.52×10^{-05}	2.69×10^{-05}	5.18×10^{-05}
ΣSO_4	4.00×10^{-18}	3.44×10^{-22}	1.83×10^{-19}
ΣH_2S	3.43×10^{-11}	1.02×10^{-03}	1.12×10^{-02}
Mg	2.54×10^{-03}	9.51×10^{-08}	6.26×10^{-04}
Ca	3.46×10^{-02}	9.77×10^{-02}	4.26×10^{-02}
Al	7.62×10^{-07}	4.49×10^{-04}	1.57×10^{-05}
Si	3.82×10^{-07}	1.17×10^{-04}	2.31×10^{-02}
Na	5.01×10^{-01}	5.12×10^{-01}	9.90×10^{-01}
Cl	5.76×10^{-01}	5.88×10^{-01}	$1.09 \times 10^{+00}$
Fe	5.54×10^{-07}	1.75×10^{-04}	3.67×10^{-03}
Cu	7.17×10^{-08}	1.24×10^{-08}	1.53×10^{-04}
Zn	2.07×10^{-04}	6.73×10^{-08}	5.27×10^{-04}
Pb	5.22×10^{-07}	2.10×10^{-10}	7.90×10^{-06}
pH	6.703	9.733	4.770

Table 2. Variations in the temperature of the hydrothermal fluid during its adiabatic cooling

Root zone type	Root zone depth, km	T_{ini}, °C	P_{ini}, kbar	P_{ini}, kbar	T_{fin}, °C
C	2	107	1.14	0.4	84.44
B	3	151	1.46	0.4	121.70
A	11	500	4	0.4	365.18

$PbCl_4^{-2}$, $Pb(HS)_2^0$, $Pb(HS)_3^-$, Pb^{+2}, $PbCl^+$, $PbCl_2^0$, $PbCl_3^-$, PbO^0, $PbOH^+$, $FeCl^+$, Fe^{+3}, Fe^{+2}, $FeCl^{+2}$, $FeCl_2^0$, FeO^0, FeO^+, FeO_2^-, $FeOH^+$, $FeOH^{+2}$, $HFeO_2^-$, and $HFeO_2^0$. The complexes were treated with the use of parameters in the HKF model compiled from (Shock et al., 1997; Sverjensky et al., 1997). These parameters were made consistent with the database in (Johnson et al., 1992), which serves as the basis for thermodynamic information in GEOCHEQ.

Effect of Adiabatic Fluid Expansion

Within the scope of the model discussed herein, the addition of lower temperature fluid in the conduit can be neglected because of the significant difference in the velocities of solutions in the down- and upwelling limbs of the system. We assumed that the ascent of fluid from the root zone to discharge zone is so fast that it is practically not associated with heat exchange with the wall rocks (Grichuk, 2000), i.e., this process can be treated as isentropic (Bishoff and Pitzer, 1985). It was also assumed that chemical interactions between the fluid and wall rocks during such a fast process can be neglected, too, and one should only take into account the precipitation of material from the cooling solution and the possible boiling of the latter.

In order to calculate the adiabatic decrease in the fluid temperature, we applied the International System of Equations 1995 (IAPWS-95) for the properties of water and water vapor, which was proposed for calculations in industrial processes (Wagner and Pruss, 2002); a software package for calculations by this system of equations was made available to us by courtesy of V.B. Polyakov (Institute of Experimental Mineralogy, Russian Academy of Sciences). The calculations were carried out in two stages: first the entropy was calculated from the initial temperature and pressure (those in the root zone), and then the temperature of the aqueous fluid in the discharge zone was calculated from the final pressure (P = 0.4 kbar, hydrostatic pressure at a depth of 4 km in an ocean) and entropy. The calculated temperature values in the discharge zone for various data points of the root zone are listed in Table 2.

The simulation tool applied in these calculations allowed us to model (with a certain accuracy) the phase separation of the hydrothermal aqueous salt fluid, including that without dissolved gases. However, the pressure P = 0.4 kbar assumed for the discharge zone is higher than the critical pressure of water, and thus, no vapor phase could be generated. Hence, phase separation in our model could involve only the degassing (release of dissolved gases) of the hydrothermal fluid. It should be mentioned that this process also contributed to the adiabatic temperature decrease, but this effect was ignored.

Evaluation of the Concentrations of Ore Components in the Fluid in the Root Zones

It was assumed in the model that the only source of Zn, Cu, and Pb in the system is olivine in the peridotites; this mineral contains the following trace amounts of the elements: 45 ppm Zn, 10 ppm Cu, and 0.28 ppm Pb (B.A. Bazylev, personal communication). Because of this, the uptake of these elements in the downwelling limb was controlled by the olivine amount dissolved in each block. It was determined that the addition of ore elements to hydrothermal fluid first increases in the course of its percolation down the vertical section of the rocks (to 129°C) at an increase in the dissolution rate of olivine. At greater depths, at temperatures of 107–239°C, the scavenging of these elements from the rocks drastically diminishes, because olivine is practically completely dissolved at this level by the earlier fluid portion (wave). Further fluid transport along the downwelling limb of the hydrothermal system (261–416°C) is, again, associated with an increase in the uptake of

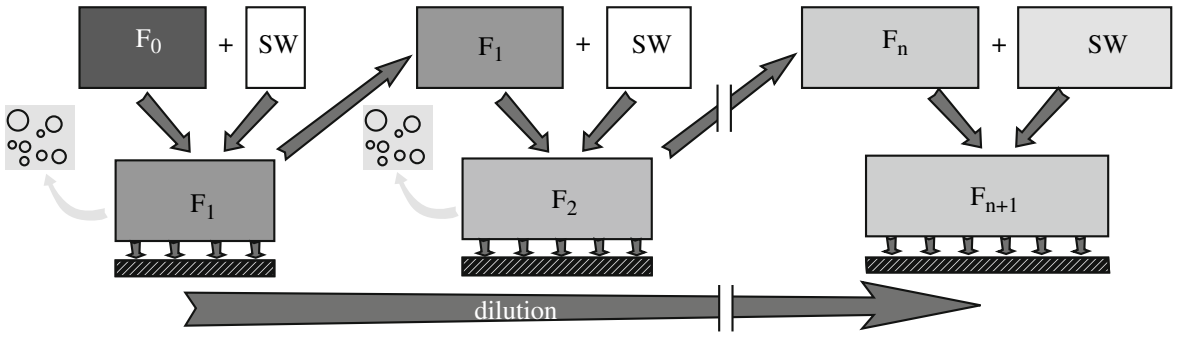

Fig. 2. Assumed model pattern for the successive dilution of the hydrothermal fluid with seawater in the discharge zone.

the elements due to intense olivine dissolution. The further passage of the elements into solution in the deepest (near the roots) zone of the circulation cell at 438–484°C is blocked by olivine stability at those *P–T* conditions.

Calculations indicate that fluid becomes oversaturated with respect to ore component at a certain level of the downwelling limb, and hence, much ore material is redeposited there in the wall rocks. This process gives rise to disseminated ore mineralization (sphalerite, chalcosine, galena, and native copper) typical of many serpentinized abyssal peridotites. In the upper portion of the simulated vertical section (≤107°C), Zn and Pb remain dissolved in the fluid. At higher temperatures (129–284°C), the hydrothermal fluid looses practically all ore elements contained in it, and at lower levels, at temperatures up to 438°C, the passage of ore material into the fluid is resumed. This provides insight into the mobilization and redeposition of ore material at the downwelling limb of the hydrothermal system that controls the possible ore potential of hydrothermal fluid in the root zone. The ratio of the mass of ore material that passed into fluid at the upwelling limb of a high-temperature hydrothermal system to the total mass of material dissolved at the downwelling limb is 7.5% for Zn, 9.5% for Cu, and 57.3% for Pb.

RESULTS OBTAINED BY SIMULATING PHASE TRANSFORMATIONS AND MATERIAL BALANCE AT THE UPWELLING LIMBS OF HYDROTHERMAL SYSTEMS IN PERIDOTITES AT SLOW-SPREADING MID-OCEANIC RIDGES

Hydrothermal System with a Root Zone A (T = 500°C, P = 4 kbar)

In this block of the model, we consider the variant of the upwelling limb of a hydrothermal system with the deepest root zone (at approximately 11 km). Where discharged from the vent, the hydrothermal fluid had in this variant a temperature of 365°C (Table 2).

Fluid evolution and mineral-forming processes in fluid conduits. Calculations indicate that 1 kg of fluid ascending to the mouth of a conduit in a high-temperature hydrothermal system releases 0.08 mol of gases (11 cm^3 at a pressure of 0.4 kbar). The gas is dominated by hydrogen (70%) and water vapor (30%). The ascent of the fluid is associated with the crystallization of quartz (which is predominant), daphnite, talc, and pyrrhotite. These phases obviously determine the mineralogy of the walls of fluid conduits in the high-temperature hydrothermal system. For this system we have also analyzed the variations in the produced mineral assemblages in the walls of the fluid conduit with time. To do this, in addition to the second wave, we modeled the successive introduction of additional fluid portions into the conduit; these portions were obtained from the downwelling limb at waves 9–10 (Silantyev et al., 2009). The fluid precipitated daphnite and tremolite. This allowed us to evaluate the character of zoning in the walls of the fluid conduit in the high-temperature hydrothermal system hosted by peridotites. The zoning consisted of the following two mineral assemblages: *Qtz* + Fe-*Chl* + *Tlc* + *Po* (older zone, outer with respect to the conduit) ⟶ Fe-*Chl* + *Tr* (younger inner zone). [1]

Fluid evolution and mineral-forming processes in the discharge zone. The mixing of the hydrothermal fluid and seawater was simulated as a series of successive additions of gradually increasing seawater portions to the fluid. The minerals crystallizing during each of the mixing stages were removed from the system. Mixing was associated with the release of gases, which were also removed from the system (Fig. 2).

In the discharge zone of high-temperature hydrothermal fluid, its mixing with seawater is accompanied by a progressive decrease in the temperature of the mixture and the precipitation of minerals in the following sequence (Figs. 3, 4):

[1] Mineral symbols: *Anh*—anhydrite, *Arg*—aragonite, *Atg*—antigorite, *BN*—bornite, *Brc*—brucite, Ca-*Sap*—Ca-saponite, *Ccp*—chalcopyrite, *Chl*—chlorite, *Ctl*—chrysotile, *Dol*—dolomite, *Gn*—galena, *Gt*—goethite, *Hem*—hematite, *Mag*—magnetite, *Py*—pyrite, *Po*—pyrrhotite, *Qtz*—quartz, *Sp*—sphalerite, *Tlc*—talc, *Tr*—tremolite.

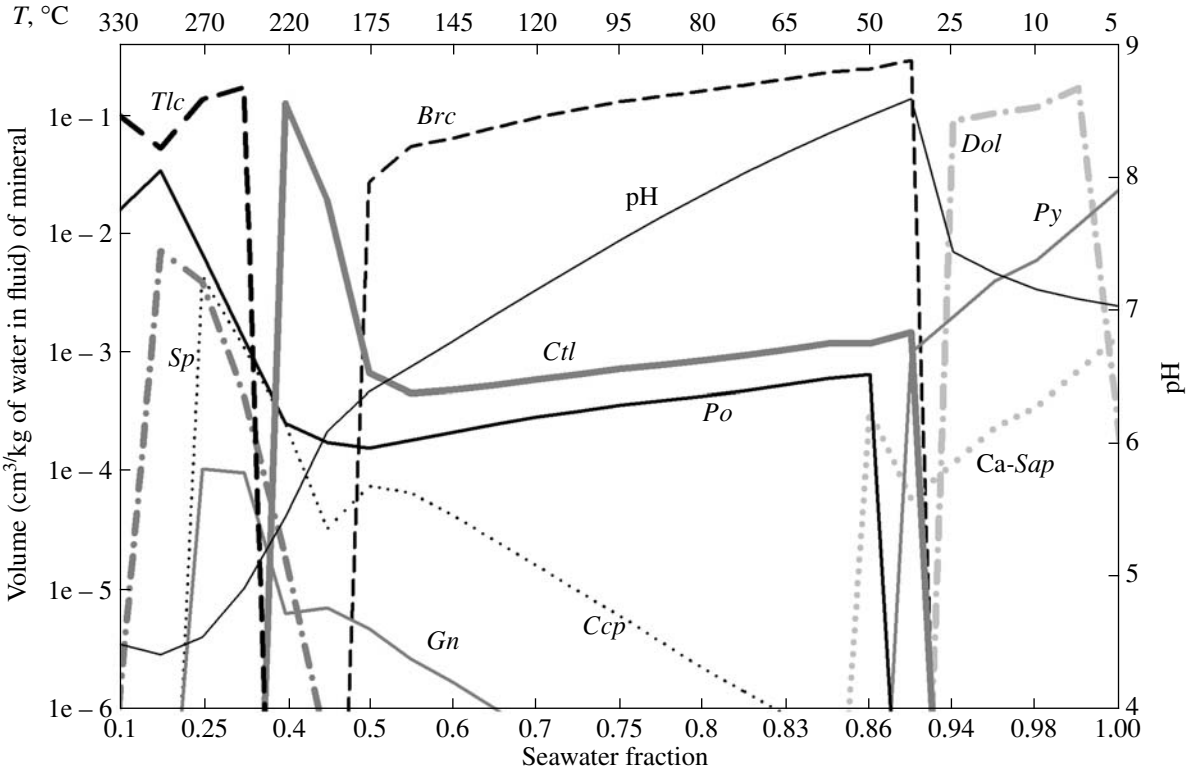

Fig. 3. Crystallization sequence of minerals in the discharge zone from high-temperature hydrothermal fluid circulating through peridotites.

T = 330–220°C (seawater fraction = 0.1–0.35) – *Sp* + *Ccp* + *Po* + *Gn* (trace amounts) + *Tlc*;

T = 220–25°C (seawater fraction = 0.35–0.90) – *Po* (trace amounts) + *Ccp* (trace amounts) + *Ctl* + *Brc* + *Sp* (trace amounts) + *Gn* (trace amounts);

T = 25–5°C (seawater fraction = 0.90–0.99) – Ca-*Sap* (appears at 50°C) + *Py* (appears at 50°C) + *Dol*.

Analysis of the simulation results indicates that the intense precipitation of sulfides during initial mixing stages (until the seawater fraction reaches 0.45) is maintained by the very high reducing potential of the initial hydrothermal fluid and the addition of seawater-derived sulfate. This led to sulfate reduction and increased the concentration of sulfide S in the mixture. Although hydrogen was spent on reduction, mixing was associated with its release into the gas phase because of a decrease in its solubility with decreasing temperature.

As follows from Fig. 3, the sharp increase in the pH from 4.7 to 6 early in the process of mixing was associated with the massive precipitation of chrysotile. The further monotonous pH increase from 6 to 8.5 was accompanied by the precipitation of chrysotile and brucite. The significant dilution of the fluid with seawater in the region of a drastic pH decrease from 8.5 to 7 was marked by the deposition of pyrite and dolomite.

It is worth mentioning that the bulk of the ore material, which consisted of sphalerite, pyrrhotite, chalcopyrite, and galena, precipitated from high-temperature hydrothermal fluid very early in the process of its mixing with seawater at temperatures of 330–250°C and a seawater fraction of 0.1–0.3 (Fig. 5). Pyrite appears in the model ore edifice only during the final stages of fluid mixing with seawater at temperatures of ≤50°C and seawater fraction of no lower than 0.85. Figure 6 shows the crystallization succession of ore minerals in the narrow region of conditions corresponding to temperatures of 362–271°C and a seawater fraction of 0.01–0.25. The crystallization sequence of ore phases during the "slow" mixing of the fluid with seawater in the high-temperature region of the system is as follows: pyrrhotite ⟶ sphalerite ⟶ bornite ⟶ chalcopyrite + galena (Fig. 6).

Crystallization from pure seawater at its heating near a hydrothermal vent. In modeling the precipitation succession of minerals in the discharge zone of high-temperature hydrothermal fluid, one should necessarily consider the contribution of precipitation from "pure" seawater heated near a hydrothermal vent. Our

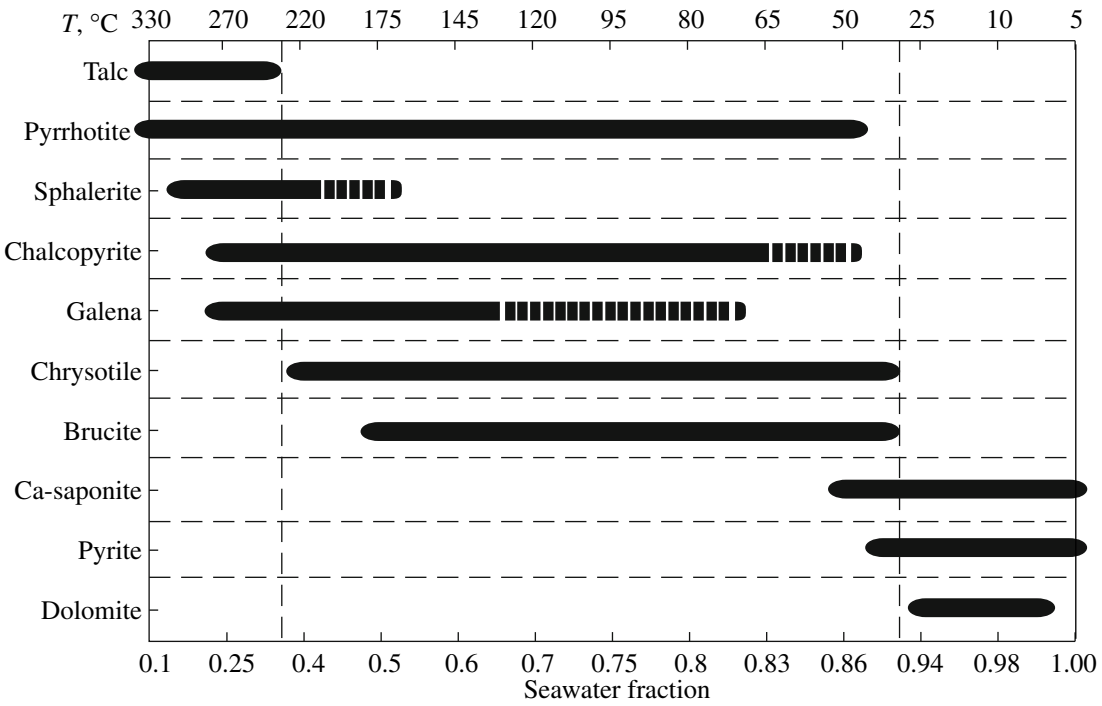

Fig. 4. Temperature mineral zoning in a high-temperature hydrothermal edifice on serpentinite.

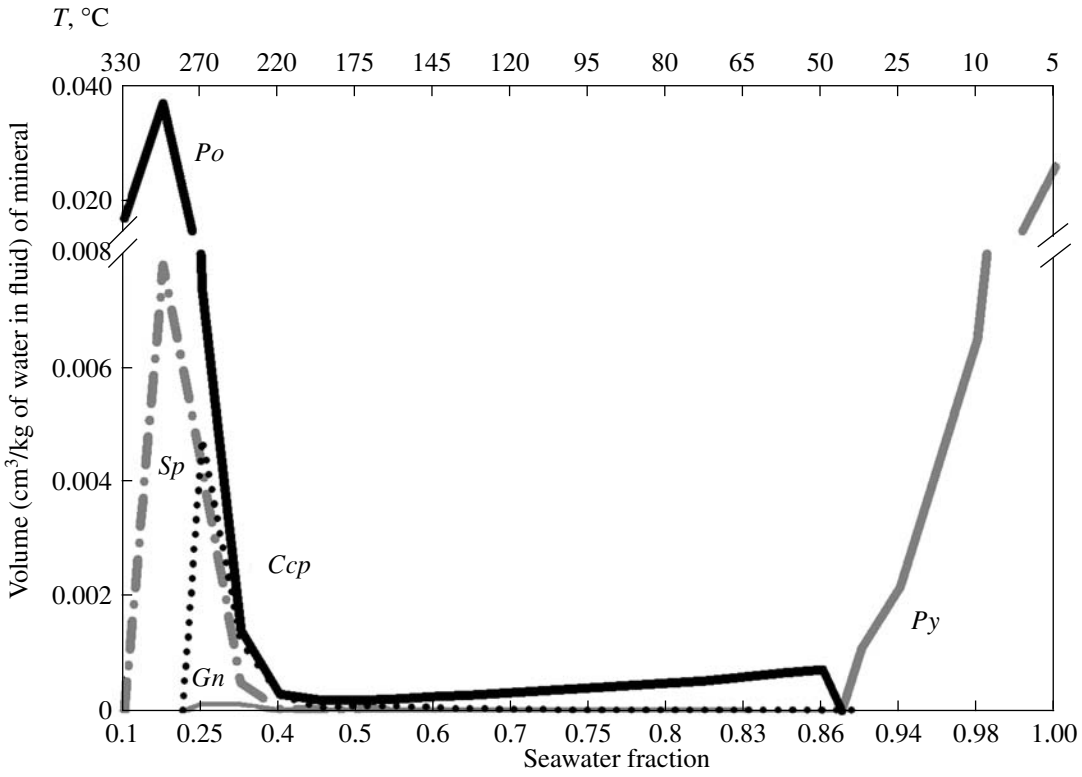

Fig. 5. Crystallization sequence of ore minerals from high-temperature hydrothermal fluid circulating through peridotites during the growth of a hydrothermal edifice.

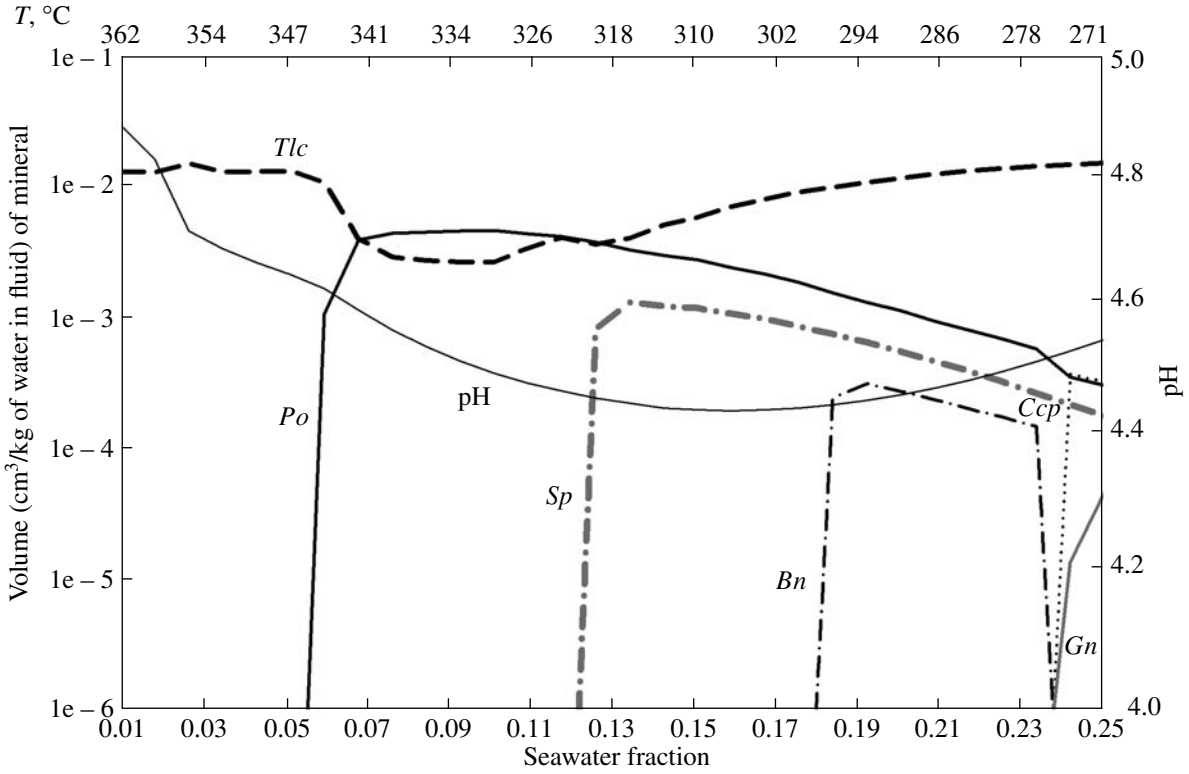

Fig. 6. Crystallization sequence of minerals in the high-temperature zone of fluid and seawater mixing from high-temperature hydrothermal fluid.

simulation results show that seawater heating to 365°C is accompanied by the successive crystallization of the following mineral phases (Fig. 7): at ≤145°C: dolomite + goethite (the latter gives way to hematite at $T > 70$°C) + Ca-saponite (at $T \le 75$°C); at 150–235°C: anhydrite + magnesite (predominant) + hematite + calcite; at 235–365°C: anhydrite + brucite (predominant) + antigorite + hematite + chlorite. As the temperature increases and minerals crystallize from seawater, its pH monotonously decreases from 6.8 to 5.3.

Zoning of hydrothermal products in the discharge zone of the high-temperature hydrothermal fluid. The crystallization succession of minerals presented above can be paralleled with the following mineralogical zoning of the conduits and edifices in high-temperature hydrothermal systems.

When fluid moves through conduits, mineral zoning is formed that typically has an outer ore (pyrrhotite-bearing) quartz–sulfide outer zone, which contains Fe-talc and Fe-chlorite, and an inner barren zone, which can likely develop at long-lived fluid conduits. The discharge zone of the hydrothermal fluid is characterized by conditions favorable for the growth of ore chimneys, whose zoning reflects the lateral temperature decrease and a change in the fluid composition when it mixes with seawater. The zoning is as follows: pyrrhotite + sphalerite (inner highest temperature zone of the edifice) ⟶ sphalerite + bornite + chalcopyrite + subordinate galena (intermediate high-temperature zone); this zone contains talc. The next (outer) higher temperature zone consists of serpentine and brucite with minor amounts of ore minerals. Finally, the fourth (highest temperature) zone is made up of dolomite, saponite, and pyrite. Obviously, pyrite crystallization from heated seawater results in that the aforementioned zones of the hydrothermal edifice contain anhydrite, brucite, calcite, chlorite, hematite, goethite, and dolomite, which can fill cavities in the walls of hydrothermal chimneys of smokers, compose outer crusts of these chimneys, and can be present in the hydrothermal precipitates of the discharge zones.

Hydrothermal System with a Root Zone B (T = 151°C, P = 1.4 kbar)

In this variant of the upwelling limb of a hydrothermal system, the depth of the root zone is close to 3 km. When discharged from the vent, the hydrothermal fluid has a temperature of 122°C due to adiabatic cooling. Fluid scent is not associated with either gas release or any significant precipitation of minerals (only small amounts of daphnite crystallize).

Fluid evolution and mineral-forming processes in the discharge zone. Our simulations demonstrate that the discharge zone of a low-temperature fluid is characterized by qualitatively different mineral-form-

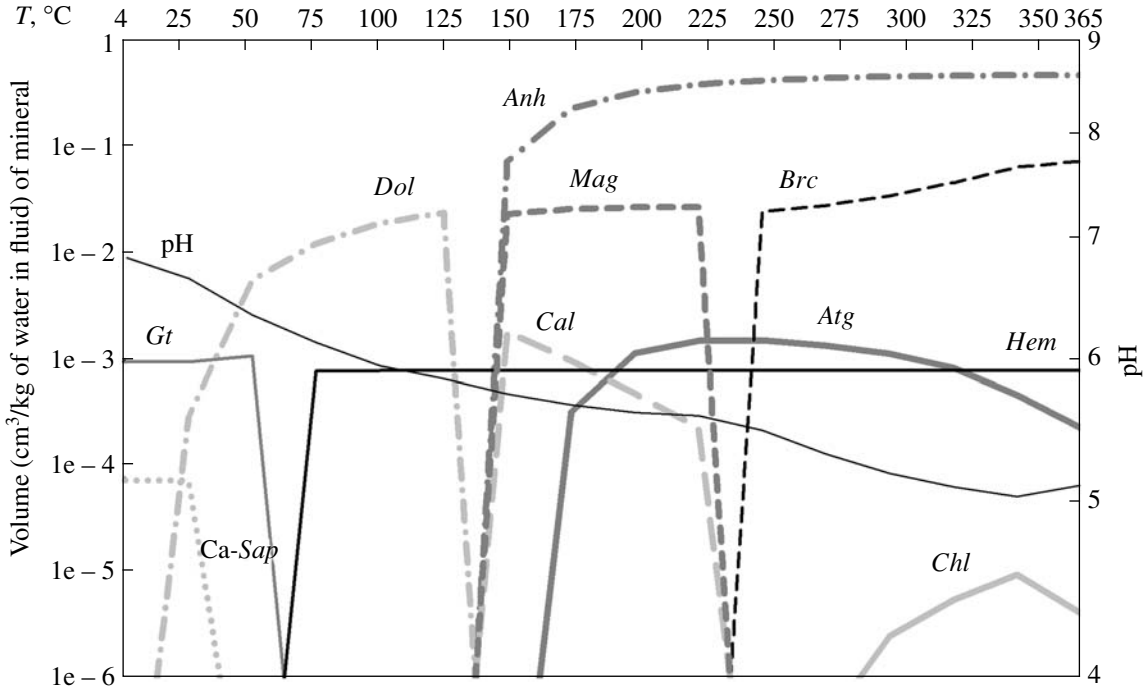

Fig. 7. Crystallization sequence of minerals from pure seawater in the discharge zone of high-temperature hydrothermal fluid.

ing processes than those in the high-temperature system. Fluid mixing with seawater in this zone and the corresponding temperature decrease bring about the following precipitation succession of minerals (Figs. 8, 9):

T = 110–90°C (seawater fraction = 0.1–0.30) – *Brc* (predominant) + *Chl* (daphnite, which gives way to clinochlore at 100°C) + *Po* (minor amounts) + *Sp* (trace amounts) + *Gn* (trace amounts);

T = 90–58°C (seawater fraction = 0.30–0.53) – *Brc* + Ca-*Sap* (both phases are predominant) + *Chl* (clinochlore) + *Py* + *Sp* (trace amounts) + *Ccp* (trace amounts);

T = 58–5°C (seawater fraction = 0.53–0.99) – *Dol* + Ca-*Sap* (both phases are predominant) + *Py*.

The moderately low-temperature hydrothermal system is principally different from the high-temperature one in the character of pH variations in the hydrothermal fluid during its mixing with seawater. Figure 8 demonstrates that pH remains high (close to 10.5) at temperatures from 110 to 65°C and rapidly decreases starting at a temperature of 65°C to 7.2 at 40°C (seawater fraction is 0.7). The further cooling of the fluid is associated only with an insignificant pH decrease to 6.8. The aforementioned principal decrease in the pH of the mixture corresponds to the onset of dolomite precipitation and the termination of brucite crystallization.

Inasmuch as the concentrations of ore elements in the moderately low-temperature fluid are very low, fluid mixing with seawater did not result in the precipitation of any significant amounts of sulfides. The hydrothermal edifices are dominated in this instance by nonore minerals.

Zoning of hydrothermal products in the discharge zone of the moderately low-temperature hydrothermal fluid. It follows from our simulation results that fluid conduits at moderately low temperature hydrothermal systems are devoid of zoning. When fluid flows through the conduits, only minor amounts of chlorite can be deposited on the walls, and no ore mineralization is formed.

Judging from our simulation results, the zoning of the hydrothermal edifices is determined by the following characteristic mineral associations: outer zone—brucite + Fe-chlorite + subordinate pyrrhotite; intermediate zone—brucite + Mg-chlorite + calcite + pyrite; outer zone—dolomite + Ca-saponite + pyrite. Ore phases are contained in all of the three zones in very low concentrations. The material precipitating from seawater at temperatures of ≤110°C may be contained in the hydrothermal edifices in the form of crusts and

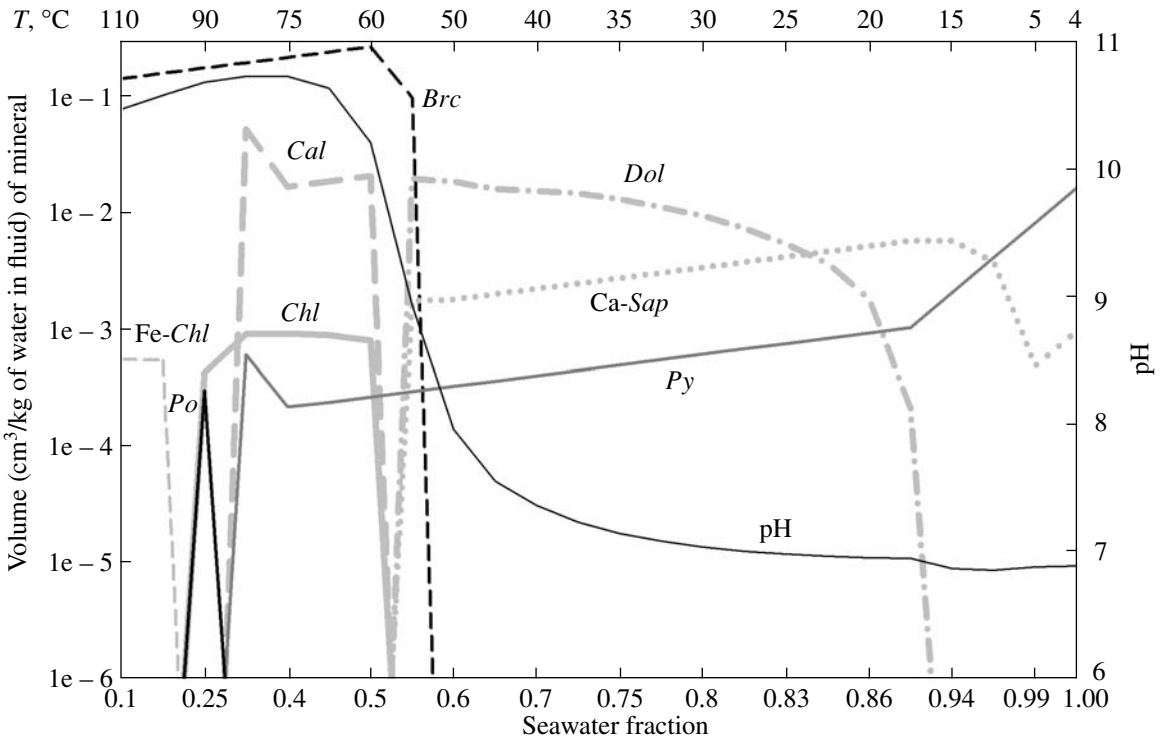

Fig. 8. Crystallization sequence of minerals in the discharge zone from a moderately low-temperature hydrothermal fluid circulating through peridotites.

hydrothermal precipitates (composed of hematite, goethite, Ca-saponite, and dolomite) (Fig. 7).

Hydrothermal System with a Root Zone C (T = 107°C, P = 1.14 kbar)

The conditions considered in this variant correspond to fluid ascent from the root zone at a depth of approximately 2 km in the vertical rock section. When outpouring from the conduit, the fluid had a temperature of 84°C.

In contrast to the two modeling variants discussed above (Fig. 1, variants A and B), no mineral-forming processes occur in the fluid conduit due to the low concentrations of dissolved ore and major component and because of the insignificant temperature change.

When the fluid mixes with seawater, the following two mineral associations successively precipitate from the low-temperature and weakly mineralized fluid coming from the shallow-depth root zone: (1) T = 76.4–56.8°C (seawater fraction is 0.1–0.34)—dolomite (predominant) + sphalerite + hematite; and (2) $T \le 51.5$°C (seawater fraction is 0.41–1)—dolomite (predominant) + goethite + Ca-saponite. The pH of the fluid is close to 6.5 throughout the whole temperature range. The total volume of the low-temperature mineralization produced by the precipitation of material from the low-temperature fluid does not exceed 0.007 cm^3/kg of water of the fluid, and the predominant source of the precipitating material is seawater. In the discharge zone of the upwelling limb at the seafloor surface, the low-temperature hydrothermal fluid is depleted in Mg, Si, Fe, S, and C relative to seawater but is enriched in Ca, Zn, and Pb. The concentration level of gases dissolved in the fluid of the low-temperature model system is close to that typical of seawater.

MODEL VERIFICATION

The comparison of our aforementioned simulation results for the upwelling limb of a hydrothermal system in peridotites with the mineralogy of ore edifices and with the physicochemical parameters of hydrothermal vents typical of such hydrothermal fields as Ashadze, Logachev, Lost City, Rainbow, and Saldanha allowed us to identify major physicochemical factors that control the differences between these naturally occurring hydrothermal fields.

The character of the simulated crystallization succession of minerals in the conduits and discharge zone of the high-temperature (365°C) hydrothermal fluid and the related zoning of the conduits and hydrothermal edifices are generally similar to the major features of natural edifices and conduits at high-temperature hydrothermal fields on serpentinized peridotites at MAR: Ashadze—the temperature of the outpouring fluid is 355°C (*Shipboard…*, 2007), Logachev—346°C (*Shipboard…*, 2007), and Rainbow—365°C (Douville et al., 2002). Active ore chimneys at the Ashadze field

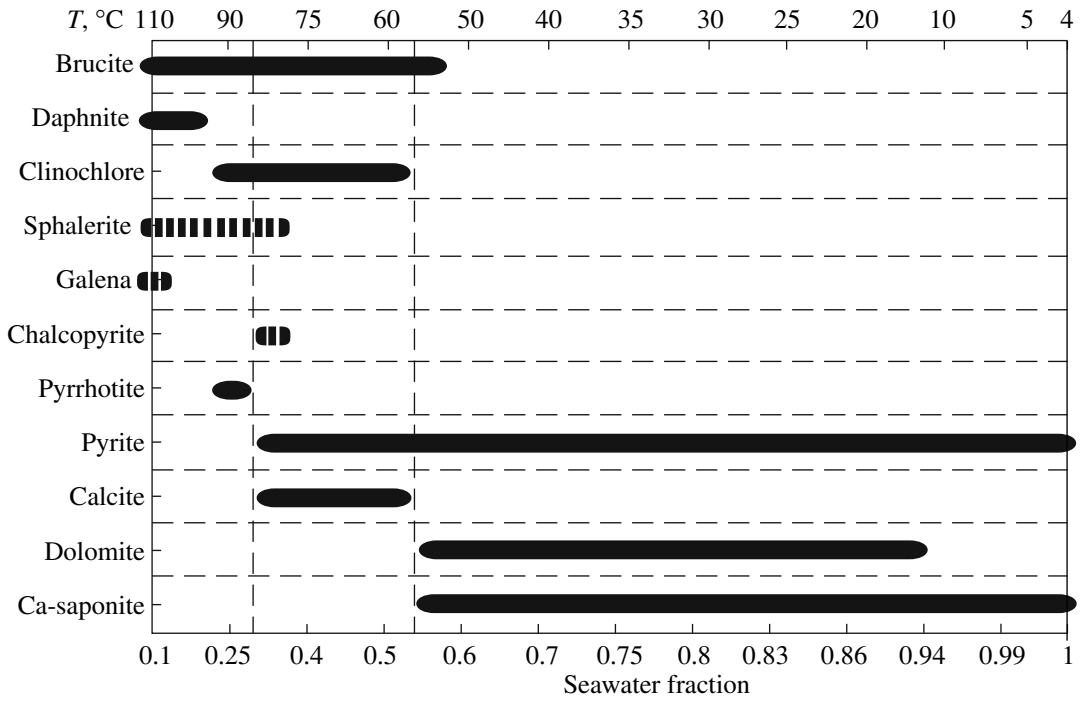

Fig. 9. Temperature mineral zoning in a moderately low-temperature hydrothermal edifice on serpentinite.

show the following zoning patterns of ore mineral associations: sphalerite + Cu–Fe sulfides (inner zone) ⟶ pyrrhotite + chalcopyrite + isocubanite (intermediate zone) ⟶ sphalerite (outer zone) (*Shipboard…*, 2007). Ore edifices at the Logachev field consist of chalcopyrite, sphalerite, isocubanite, and anhydrite; the surface of the ore chimneys is covered with Fe hydroxides (*Shipboard…*, 2007). Active sulfide edifices at the Rainbow field are zonal and consist of chalcopyrite and sphalerite (predominant)—inner zone; chalcopyrite, cubanite, sphalerite, and bornite—outer zone (Vikent'ev, 2004). As is mentioned in (Vikent'ev, 2004), sulfide aggregates in active chimneys at the Rainbow field is anhydrite, which is unevenly distributed in the material composing the walls of the ore edifices. The temperature crystallization sequence of ore minerals obtained by means of numerical simulations consists of a high-temperature (older) association of pyrrhotite, chalcopyrite, and sphalerite and a younger association with pyrite; analogous associations were mentioned in the schematic structure of the active portion of the Rainbow field in (Marques et al., 2006).

Bogdanov et al. (2006) reported data testifying that the walls of fluid conduits at the Logachev field typically consist of amorphous silica and sulfides. An analogous mineral association was obtained in our numerical simulations for the outer (relative to the fluid conduit) zone of the high-temperature model system.

Mineral zoning around fluid conduits of hydrothermal systems in serpentinites is characterized by the presence of talc in the ore (pyrrhotite-bearing) quartz–sulfide outer zone. Bach and Klein (2007) discussed the results obtained on the mineralogy of deep-sea drilling core (ODP, Leg 209, Hole 1268) that recovered peridotites with abundant talc from the intersection area of MAR and 15°N Fracture Zone, which includes a large hydrothermal cluster in the area of the Ashadze and Logachev fields. Bach and Klein (2007) believe that talc crystallization in peridotites at MAR requires that the hydrothermal system involved an aqueous fluid with a high silica activity. This chemical feature of hydrothermal fluid at the upwelling limb of the high-temperature system was inferred from both direct observations and results of numerical simulations.

Hydrothermal precipitates at active hydrothermal fluids in peridotites in the Central Atlantic typically contain goethite and nontronite (Bogdanov et al., 2006). It should be mentioned that, similar to saponite, nontronite yielded by our simulations for the high-temperature hydrothermal system belongs to the montmorillonite group (smectites) and can thus be regarded as its naturally occurring analogue. Hence, it is reasonable to suggest that low-temperature hydrothermal precipitates at active fields on serpentinites are formed predominantly by the precipitation of material at $T \le 75$°C from pure seawater heated in the discharge zone of the hydrothermal fluid.

Hydrothermal fluid coming to the seafloor surface at the Rainbow hydrothermal field has a very high concentrations of dissolved silica (see, for example, Seyfert et al., 2005). It is worth mentioning that simulations for the upwelling limb of the high-temperature hydro-

thermal system also yielded a high initial silica concentration in the fluid in the discharge zone, and this value was close to those measured at hydrothermal vents at Rainbow. It should, however, be mentioned that the pH value (4.5) calculated in the model for the high-temperature fluid discharged at the upwelling limb of the hydrothermal system is higher than that measured in situ in hydrothermal vents at Rainbow (2.8 (Douville et al., 2002)) and corresponds to the pH level at the Ashadze (pH 3.9–4.1; *Shipboard…*, 2007) and Logachev (pH 4.3–4.9; *Shipboard…*, 2007) fields.

The simulation results reported in this publication for the high-temperature upwelling limb of a hydrothermal system in serpentinites are generally consistent with the aforementioned empirical data on the mineralogy of fluid conduits, ore edifices, and physicochemical parameters of fluid at high-temperature hydrothermal fluids in MAR peridotites. Our simulation results suggest that the root zone feeding hydrothermal systems at the Ashadze, Logachev, and Rainbow fields is located at the bottom of the crustal section, at a depth of approximately 11 km.

Our simulation results for the moderately low-temperature hydrothermal system reproduce a situation similar to that at the development of the Lost City hydrothermal system. In our simulations, the fluid coming from the root zone hosted in serpentinites at a depth of 3 km has a temperature of approximately 110°C during the very early stages of its mixing with seawater upon reaching the seafloor surface; the pH of this fluid is very high (close to 10.5), and it contains a high Ca concentration. These conditions correspond to the parameters of fluid regime in the discharge zone at the Lost City field: $T = 90$°C, pH 9–11 (Kelley et al., 2005). Spires at the Lost City field consist of brucite and aragonite, which crystallize (Kelley et al., 2005) when the warm fluid with high pH and high Ca concentrations mixes with seawater, which provides the Mg and HCO_3^- ions.

As was demonstrated above, the minerals precipitating in the model system during initial mixing stages of fluid with seawater are dominated by brucite and a carbonate phase (calcite), with the latter mineral giving way to dolomite in the course of further mixing and temperature decrease (Mg uptake from seawater). The region of parameters marked in the model system as that of brucite crystallization confirms the hypothesis in (Bach and Klein, 2007) that brucite is formed in hydrothermal systems in serpentinites from moderately low-temperature fluid with high pH and a low silica activity. The silicate phases (daphnite and clinochlore) yielded by our simulations account for a very low fraction of the minerals precipitating from the fluid, and ore phases are contained in this material only in trace amounts. The crystallization sequence of minerals obtained in our simulations for hydrothermal edifices in a moderately low-temperature discharge zone of hydrothermal fluid is obviously similar to the hydrothermal material recovered from the Lost City field. The simulation results also imply that fluid conduits in such hydrothermal systems are devoid of any traces of zoning, and the ore mineralization typical of the high-temperature system is absent. In this context it is pertinent to recall that the vein suite in the serpentinites hosting the Lost City field consists of the barren serpentine–brucite–aragonite association, which could be produced by the precipitation of mineral material during the flow and cooling of moderately low-temperature fluid with high pH and a high Ca concentration. With regard for the data presented above, it is reasonable to hypothesize that the root zone of the circulation hydrothermal cell at the Lost City field is hosted in peridotites and occurs at a depth of no more than 3 km, and the fluid has a temperature of approximately 150°C at that depth level.

The mineralogical and geochemical effects obtained by simulating the upwelling limb of the low-temperature hydrothermal system (the temperature of the discharged fluid is 84°C) testify to an extremely low ore potential of such systems and to the absence of any pronounced hydrothermal edifices related to them.

A possible natural analogue of our model for the low-temperature hydrothermal system is the Saldanha hydrothermal field, which is the lowest temperature among those hosted in serpentinites. Our model implies that the low-depth fluid in the discharge zone is characterized by very low concentrations of gases (for instance, methane) dissolved in it. Scarce and unsystematic information on the chemistry of fluid in low-temperature vents at the Saldanha field suggests that the composition of this fluid is close to that of seawater and that the fluid contains very little methane (Charlow et al., 1996). As in the model, the serpentinites hosting the Saldanha field contain no veins that can be interpreted as mineralized fluid conduits. The temperature of hydrothermal fluid evaluated in our simulations for the low-temperature system is 84°C, whereas the in situ measured temperature of the fluid filtering through the thin foraminiferal ooze layer covering the serpentinite massifs at Saldanha seamount does not exceed 7–9°C (Dias and Barriga, 2006). However, these authors suggested that a fluid of higher temperature than that measured at its discharge site can be also involved in the hydrothermal system at Saldanha, and this fluid can be captured in voids and conduits below the sediments. Similar to the hydrothermal mineral association in hydrothermal precipitates and microedifices at the Saldanha field, the model low-temperature hydrothermal system is characterized by the presence of sphalerite and Ca-saponite (the material from the Saldanha field contains nontronite). As was demonstrated in (Silantyev et al., 2009), the serpentinization of mantle rocks in slow-spreading ridges becomes efficient starting at a temperature of 107°C. It is worth mentioning that this temperature in our model corresponds to hydrothermal fluid in the root zone of the low-temperature hydrothermal cell. Conceivably, heat is provided for low-temperature hydrothermal fields (such as

Saldanha) by exothermal serpentinization reactions of peridotites in slow-spreading MOR. Our simulation results for the upwelling limb of the hydrothermal system with a shallow-depth and low-temperature root zone can be readily applied in reproducing the conditions under which hydrothermal fluids ascend to the seafloor surface at the Saldanha field.

Our comparative analysis of natural observations and results of numerical simulations led us to conclude that the specifics of the ore mineralization and geochemistry of hydrothermal fluids coming into the discharge zones of hydrothermal fields hosted in peridotites are controlled, first of all, by the temperature in the root zones of the hydrothermal systems.

CONCLUSIONS

Our results obtained by means of the numerical simulations of the upwelling limb of hydrothermal circulation cells hosted in serpentinites remarkably append our earlier model for the development of hydrothermal systems in peridotites in slow-spreading ridges (Silantyev et al., 2009). The synthesis of simulation data obtained in the course of our research for the downwelling limb of the hydrothermal system and data presented above for the upwelling limb of the same system led us to formulate the following principal conclusions that are important for evaluating the ore potential and geochemical specifics of hydrothermal fields on the Hess crust:

(1) Ore material is accumulated in the discharge zones of hydrothermal systems hosted in serpentinites only at a high temperature of the fluid discharged at the upwelling limb of the circulation cell. Obviously, hydrothermal fields at which this condition is observed have a root zone situated at a significant depth in the crustal section.

(2) A significant volume of ore material involved in hydrothermal exchange between the peridotites and fluid is redeposited at the downwelling limb of the hydrothermal system and gives rise to disseminated ore mineralization typical of many serpentinized abyssal peridotites.

(3) The ratio of the volume of the ore material introduced into the upwelling limb of the hydrothermal system to the total volume of the material dissolved at the downwelling limb is 7.5% for Zn, 9.5% for Cu, and 57.3% for Pb.

(4) Inasmuch as plutonic complexes hosting all high-temperature hydrothermal fields at MAR contain an association of peridotite and gabbro (Ashadze, Logachev, and Rainbow fields), it is reasonable to suggest that the peridotite–gabbro ensemble is indicative of ore mineralization related to the discharge of the high-temperature hydrothermal fluid. Conceivably, the main heat source in such hydrothermal systems is gabbroid intrusions in their root zones.

(5) The root zone of a circulation hydrothermal cell of the unique Lost City field likely occurs in peridotites at a depth of no more than 3 km, and the fluid has a temperature of approximately 150°C at this depth level.

(6) The activity of moderately low-temperature hydrothermal systems in peridotites does not result in the accumulation of ore material in the discharge zones and the growth of ore edifices.

ACKNOWLEDGMENTS

The authors thank V.B. Polyakov (Institute of Experimental Mineralogy, Russian Academy of Sciences) for consultations and for providing a computer software package that was applied in simulating the adiabatic cooling of the fluid. Data on the concentrations of ore elements in spinel peridotites from MAR were made available to us by courtesy of B.A. Bazylev (Vernadsky Institute of Geochemistry and Analytical Chemistry, Russian Academy of Sciences). This study was financially supported by the Russian Foundation for Basic Research (project nos. 06-05-64003, 08-05-00164a) and the program "Fundamental Problems of Oceanology: Physics, Geological, Biology, and Ecology" (project "Interaction of Magmatic and Hydrothermal Systems in the Oceanic Lithosphere and Mineral Resources") of the Presidium of the Russian Academy of Sciences.

REFERENCES

1. W. Bach and F. Klein, "Silica Metasomatism of Oceanic Serpentinites," in *Proceedings of 17th Goldschmidt Conference, Bremen, Germany, 2007* (Bremen Univ. Bremen, 2007), p. A48.
2. J. L. Bischoff and K. S. Pitzer, "Phase Relations and Adiabats in Boiling Seafloor Geothermal Systems," Earth Planet. Sci. Lett. **75** (4), 327–338 (1985).
3. Yu. A. Bogdanov, *Manifestations of Hydrothermal Activity in the Mid-Atlantic Ridge* (Nauchnyi Mir, Moscow, 1997) [in Russian].
4. Yu. A. Bogdanov, A. P. Lisytsin, A. M. Sagalevich, and E. G. Gurvich, *Hydrothermal Ocean Floor Ore Formation* (Nauka, Moscow, 2006) [in Russian].
5. J.-L. Charlou, H. Bougault, Y. Fouquet, et al., "Methane Degassing, Hydrothermal Activity and Serpentinization between the Fifteen-Twenty Fracture Zone Area and the Azores Triple Junction Area (Mid-Atlantic Ridge)," in *Fara Meeting, Mid-Atlantic Ridge Symposium, Reykjavik, Iceland, 1996* (Reykjavik, 1996), pp. 771–772.
6. A. S. Dias and J. A. S. Barriga, "Mineralogy and Geochemistry of Hydrothermal Sediments from the Serpentinite-Hosted Saldanha Hydrothermal Field (36°34′N; 33°26′W) at MAR" Mar. Geol. **225** (1–4), 157–175 (2006).
7. E. Douville, J. L. Charlou, E. H. Oelkers, et al., "The Rainbow Vent Fluids (36 Degrees 14′N, MAR): the Influence of Ultramafic Rocks and Phase Separation on Trace Metal Content in Mid-Atlantic Ridge Hydrothermal Fluids," Chem. Geol. **184**, 37–48 (2002).

8. E. O. Dubinina, I. V. Chernyshev, N. S. Bortnikov, et al., "Isotopic–Geochemical Characteristics of the Lost City Hydrothermal Field," Geokhimiya, No. 11, 1223–1236 (2007) [Geochem. Int. **45**, 1131–1143 (2007)].
9. G. L. Fruh-Green, D. S. Kelley, S. M. Bernasconi, et al., "30.000 Years of Hydrothermal Activity at the Lost City Vent Field," Science **301**, 495–498 (2003).
10. C. R. German and K. L. Von Damm, "Hydrothermal Processes," in *Treatise on Geochemistry* (Elsevier, New York–Boston–Sidney–Amsterdam, 2003), Vol. 6, pp. 181–222.
11. D. V. Grichuk, *Thermodynamic Models of Submarine Hydrothermal Systems* (Nauchnyi Mir, Moscow, 2000) [in Russian].
12. R. M. Haymon, "Growth History of Hydrothermal Black Smoker Chimneys," Nature **301**, 695–698 (1983).
13. J. W. Johnson, E. H. Oelkers, and H. C. Helgeson, "SUPCRT92: A Software Package for Calculating the Standard Molal Thermodynamic Properties of Minerals, Gases, Aqueous Species, and Reactions from 1 to 5000 Bars and 0° to 1000°C," Comp. Geosci. **18**, 899–947 (1992).
14. D. S. Kelley, J. A. Karson, G. L. Fruh-Green, et al., "A Serpentinite-Hosted Ecosystem: The Lost City Hydrothermal Field," Science **307** (5714), 1420–1422 (2005).
15. A. Yu. Lein, K. Yu. Bogdanova, Yu. A. Bogdanov, and L. O. Magazina, "Mineralogical and Geochemical Features of Authigenic Carbonates on Seepings and Hydrothermal Fields (By the Examples of the Black Sea Reefs and the Mounds of the Lost City Field)," Okeanologiya **47** (4), 577–593 (2007) [Oceanology **47**, 537–553 (2007)].
16. A. F. A. Marques, F. Barriga, V. Chavagnac, and Y. Fouquet, "Mineralogy, Geochemistry, and Nd Isotope Composition of the Rainbow Hydrothermal Field, Mid-Atlantic Ridge," Mineral. Deposita **41**, 52–67 (2006).
17. M. V. Mironenko, N. N. Akinfiev, and T. Yu. Melikhova, "GEOSHEQ—A Complex of Thermodynamic Modeling of Geochemical Systems," Vestn. OGGGN RAN **5** (15), 96– 97 (2000).
18. X. Peng and H. Zhou, "Growth History of Hydrothermal Chimneys at EPR 9–10°N: A structural and Mineralogical Study," Sci. China. Ser. D. Earth Sci. **48** (11), 1891–1899 (2005).
19. W. E. Seyfried, Q. Fu, and D. I. Foustoukos, "The Rainbow Hydrothermal System: Experimental and Theoretical Controls on Vent Fluid Chemistry and Subseafloor Alteration Processes," Eos Trans. AGU. Fall Meet. Suppl. Abstract. **86**, No, 52. OS21C-07 invited (2005).
20. *Shipboard Scientific Party. SERPENTINE Scientific Cruise Report. Center de Brest, France, 2007* (Iferemer—Centre de Brest, 2007).
21. E. L. Shock, E. L. Sassani, M. Willis, and D. A. Sverjensky, "Inorganic Species in Geologic Fluids: Correlations among Standard Molal Thermodynamic Properties of Aqueous Ions and Hydroxide Complexes," Geochim. Cosmochim. Acta **61**, 907–950 (1997).
22. S. A. Silantyev, M. V. Mironenko, and A. A. Novoselov, "Hydrothermal Systems in Peridotites of Slow-Spreading Mid-Oceanic Ridges. Modeling Phase Transitions and Material Balance: Downwelling Limb of a Hydrothermal Circulation Cell," Petrologiya **17** (2), 154–174 (2009) [Petrology **17**, (2009)].
23. D. A. Sverjensky, E. L. Shock, and H. C. Helgeson, "Prediction of Thermodynamic Properties of Aqueous Metal Complexes to 1000°C and 5 Kb", Geochim. Cosmochim. Acta **61**, 1359–1412 (1997).
24. M. K. Tivey, "Generation of Seafloor Hydrothermal Vent Fluids and Associated Mineral Deposits," Oceanography **20**, 50–65 (2007).
25. M. K. Tivey and R. E. McDuff, "Mineral Precipitation in the Walls of Black Smoker Chimneys: a Quantitative Model of Transport and Chemical Reaction," J. Geophys. Res. **95** (B8), 12617–12637 (1990).
26. V. I. Vikent'ev, *Genesis and Metamorphism of Sulfide Ores* (Nauchnyi Mir, Moscow, 2004) [in Russian].
27. K. L. Von Damm, L. G. Buttermore, S. E. Oosting, et al., "Direct Observation of the Evolution of a Seafloor Black Smoker from Vapor to Brine," Earth Planet. Sci. Lett. **149**, 101–112 (1997).
28. K. L. Von Damm, "Controls on the Chemistry and Temporal Variability of Seafloor Hydrothermal Fluids," in *Seafloor Hydrothermal Systems: Physical, Chemical, Biological, and Geological Interactions*, Ed. by S. E. Humphris, R. A. Zierenberg, L. S. Mullineaux, and R. E. Thomson, AGU Monogr. Ser. (Am. Geophys. Union, Washington, 1995), Vol. 91, pp. 222–247.
29. W. Wagner and A. Pruss, "The IAPWS Formation 1995 for the Thermodynamic Properties of Ordinary Water Substance for General and Scientific Use," J. Phys. Chem. Ref. Data **31**, 387–535 (2002).